CHAPTER 3

EXPERIMENTAL

Bipolar plates perform a number of functions with in the PEM fuel cell (Mehta and Cooper, 2003). They have been used to distribute the fuel and oxidant within the cell, separate the individual cells in the stack, carry current away from each cell, carry water away from each cell, humidify gases, and keep the cells cool. Plate topologies and materials facilitate these functions. Topologies can include straight, serpentine, or inter-digitated flow fields, internal manifolding, internal humidification, and integrated cooling. Materials have been proposed on the basis of chemical compatibility, resistance to corrosion, cost, density, electronic conductivity, gas diffusivity/impermeability, manufacturability, stack volume/kW, material strength, and thermal conductivity. Given the criteria found in literature, non-porous graphite, a variety of coated metals, and a number of composite materials have been suggested for used in bipolar plates.

For coated metallic plates; aluminum, stainless steel, titanium, and nickel are considered possible alternative materials for the bipolar plate in PEM fuel cells. No matter the plate configuration, because bipolar plates are exposed to an operating environment with a pH of 2-3 at high temperatures, if not designed properly, dissolution or corrosion of the metal will occur. Specifically, when the metal plate is dissolved, the dissolved metal ions diffuse into the membrane and are trapped at ion exchange cites, resulting in a lowering of ionic conductivity. In addition, a corrosion layer on the surface of a bipolar plate increases the electrical resistance in the corroded portion and decreases the output of the cell.

Because of these issues, metallic bipolar plates are design with protective coating layers. The coating for bipolar plates should be conductive and adhere to the base material properly to protect the substrate from the operating environment. There are two categories of protective coating. Carbon-base coating include: graphite,

conductive polymer, diamond like carbon, organic self-assembled mono-polymers. Metal-based coatings include: noble metals, metal nitrides and metal carbides. However, conductive oxides are interesting for this application. They usually use in photovoltaic, but we are not interested in the optical transparency. For this application, we can focus on optimizing these materials for high conductivity and corrosion resistance (Adrianowycz et al., 2008).

3.1 Thin film preparation techniques

For this work, we first study the electrical conductivity of thin film. There are three types of thin film preparation techniques with different thin film.

3.1.1 Filtered Cathodic Vacuum Arc (FCVA)

Thin films of metal-doped diamond-like carbon (Me-DLC) have been interested in their properties of good adhesion (Wei et al., 1999), high hardness (Voevodin et al., 1997), low friction coefficient (Klaffke and Skopp, 1998), high thermal stability (Fu et al., 1989) and high electrical conductivity (Bewilogua, 2000). The electrical conductivity of the film varies with amount of the incorporated metal (Frenkel, 1938; Huang et al., 2000) that enhanced by metal in the DLC film to provided extra paths for electronic transportation (Huang et al., 2000).

In this thesis, we deposit metal-doped DLC using dual source cathodic arc with Mo as a metal source and one is carbon. The pulse cathodic arc used in this work has two cathodes in one anodes body (Anders et al., 2007), representing a modified “mini gun” (MacGill et al., 1998). The cathodes are pulsed using the “triggerless” arc initiation method (Anders et al., 1998). The streaming plasma were guided and transported through a curved magnetic macroparticle filter (Bilek and Anders, 1999) into the magnetic homogenizer (Anders et al., 1996; Bilek et al.,2001) to conduct deposition. The experiment was carried out with different ratio of Mo and Carbon, and varies carbon selective bias voltage. The film resistance was measured during deposition.

Si (100) and micro glass slides with sputtered Molybdenum contacts were used as the substrate materials. The electrical contacts were made on two terminals of the glass slides by magnetron sputtering, left the center for film deposition (Byon et al., 2003). The sheet resistance was continuously recorded using two-terminal configuration. The a-C:Mo films were deposited by the pulsed dual cathode filtered cathodic arc plasma source system show in Figure 3.1. These thin films were deposited using 6.4 mm diameter cathodes, separated by 2 cm centre to centre distance. The plasma from both cathodes was entered the same macro particle filter curved duct. The filter curved duct made by a coil of 5 mm diameter copper tube with 22 turns, 7 cm in diameter. The magnetic field generated by plasma arc current. Two power supplies were used for this experiment separately for Mo and carbon sources (Anders et al., 1999). The arc pulse length and current are 5 ms, 120 A for carbon and 1 ms, 760 A for Mo respectively. The experiment setup show in Figure 3.2.

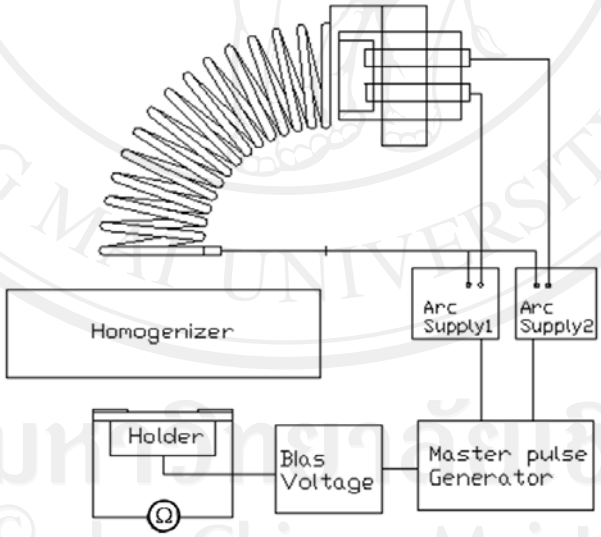

Figure 3.1 A schematic diagram of the dual sources pulsed cathodic arc.

The magnetic homogenizer was 16.7 cm inner diameter. The distance between the exit of curved filter to the magnetic homogenizer was 2 cm., and distance from the magnetic homogenizer to the substrate was 2 cm. The system base pressure was 5×10^{-6} torr; no process gas was used. The pulse repetition rate was 2 pulses per

second. The *in situ* film sheet resistance was monitored using FLUKE 189 digital multi meter connected to a computerized data acquisition system. Film resistivity was determined from the sheet resistance, $R_{\square}$, according to $\rho = R_{\square} d$, where d is the film thickness. The thickness was calibrated using by profilometry and assuming that the deposition rate per pulse is constant, i.e., pulse counting is sufficient to determine the thickness of ultrathin films.

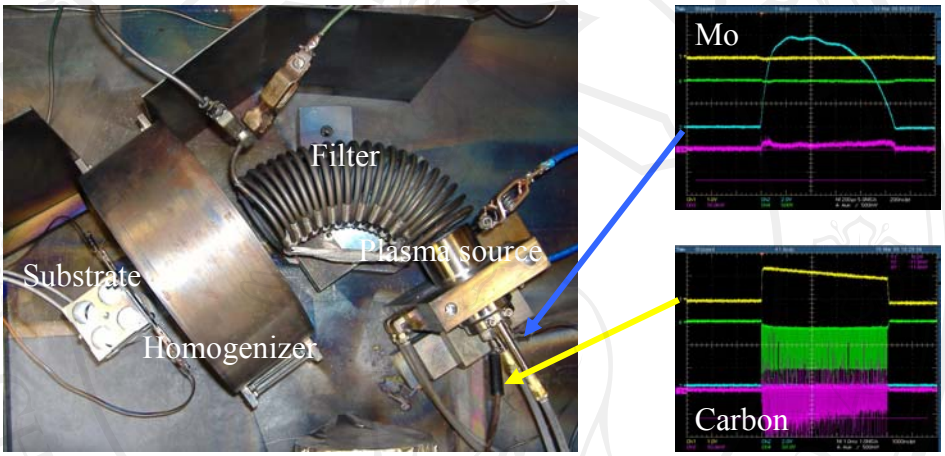

Figure 3.2 Photo of the dual sources cathodic arc plasma deposition experiment setup.

Two kinds of experiments were done. First, we varied the Mo/C pulse ratio without substrate bias. Second, the films were deposited at constant pulse ratio of Mo/C=0.05 and varied pulsed substrate bias voltage from -100 V to -1000 V, *applied to carbon only*. This could be achieved by the computerized synchronization of carbon pulses and bias power supply, which we call species-selective bias. The negative bias voltage was pulse with 25% duty cycle (4 μs on, 12 μs off). The total deposition pulse number was 2000 pulses for each film. The substrates were cleaned by ethyl alcohol and dried with a flow of pure dry nitrogen before mounting on the substrate holder. For deposition run, a witness sample of Si (100) wafer was used for profilometry, and another witness sample of borosilicate glass to be used for Raman spectroscopy.

After film deposition, the samples were left in ambient air at room temperature. Their sheet resistances were record weekly for two months to determine the stability of the films. After this period, temperature dependent measurements of the film sheet resistances were carried out in the range 300 to 515 K in ambient air. A K-type thermocouple was placed at the back of the sample to determine the temperature. Both temperature and sheet resistance were recorded during heating by FLUKE 189 digital multimeter.

The resistivity measurements (via measurements of sheet resistance and film thickness) were complimented with visible Raman spectroscopy, which would allow us to approximately deduce the sp^2/sp^3 ratio and to make tentative conclusions on the conduction mechanisms. The Raman spectroscopy was done with the 514 nm line of an argon ion laser.

3.1.2 Reactive magnetron sputtering

AISI 304 stainless steel was selected for this experiment because of its low cost and easy to find. The compositions of AISI 304 are given in table 3.1. The specimens were cut into pieces of 2×2 cm^2 with 1 mm thickness, polished with #1200 grit SiC abrasive paper and follow by one micron diamond polishing compound. The specimens were cleaned with ethanol and dried with a flow of pure nitrogen before mounting on the substrate holder. The experiments were processed in the vacuum chamber under base pressure lower than 6×10^{-6} Torr.

Table 3.1 Chemical composition of AISI 304 stainless steel (wt%).

Cr	Ni	Mo	Ti	Mn	C	Fe+other
18.45	10.54	0.00	0.00	2.00	0.07	other

Aluminum doped Zinc Oxide (ZnO:Al) film was prepared by using reactive magnetron sputtering technique. Sputtering target was a 96/4 at% of Zn/Al with 3 inch diameter. The distance between target and substrate was 13 cm. The experiment

setup was shown in figure 3.3. The MDX 500 power supply was used. Sputtering power set at 225 watts. The deposition time was 15 min. The target was cleaned by sputtering with argon for a minute before deposition. The pressure during deposition was kept at 20 mTorr. The O_2 and Ar flow were varies for different conditions.

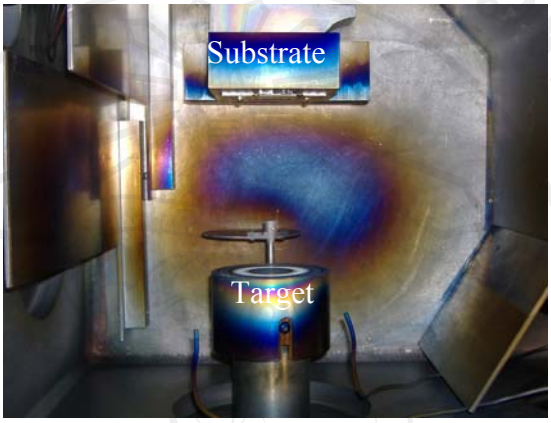

Figure 3.3 Photo of reactive magnetron sputtering setup.

ZnO thin film also conducted using reactive magnetron sputtering by Zn high purity target. Deposition condition are the same as ZnO:Al films. Si(100) with pen marked and micro glass slide with sputtered silver contacts were put with AISI 304 specimens for thickness and resistivity measurement, respectively.

3.1.3 Plasma immersion

Transition metal nitrides and carbides have been identified as candidate coating for metallic bipolar plates due to their combination of high electrical conductivity and good corrosion resistance (Baranowska and Arnold, 2006; Silva et al., 2006). Plasma nitriding is widely used for improving surface properties of ferrous and non-ferrous materials. This nitridation is an inexpensive technique and can be carried out at low temperature. Moreover, this nitridation technique can be used on complex-shaped components. Commercial AISI 304 austenitic stainless steel was used as the substrate materials. The substrate was a piece of 2×2 cm^2 with 1 mm

thickness and was cleaned before put on a stainless steel holder of 6.5 cm diameter, 2 mm thickness in the chamber. The K-type thermocouple was put under the holder to measure the sample's temperature during treatment. The experiment setup was show in figure 3.4.

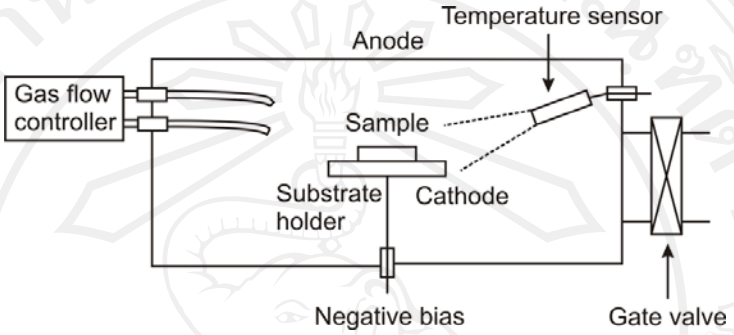

Figure 3.4 Nitridation and Carburization experiment setup.

There are four groups of nitridation and carburization experiments using different power supply and different composition gases for the best properties.

1). N_2+C_2H_2 plasma immersion.

This experiment called nitride carburization. The nitrogen (N_2) and acetylene (C_2H_2) gases were feed into the chamber. The gate valve of cryogenic vacuum pump was adjusted to control the working pressure at 60 mTorr. The negative DC voltage was applied to the holder up to 2 kV. The ratio of C_2H_2 and N_2 gas flow rate was varies. Plasma immersion was processed for 20 minute. The experimental conditions show in table 3.2.

Table 3.2 Gas flow rate in N_2+C_2H_2 plasma immersion.

Experiments	N_2 flow (sccm)	C_2H_2 flow (sccm)
Exp 118	50	10
Exp 119	50	15
Exp 120	50	5

2). Plasma nitriding by Pinnacle plus power supply.

The 4% H_2 and N_2 gas mixed was used for this experiment. The substrate holder was bias with Pinnacle plus DC pulse power supply. Power set point of the Pinnacle plus set at 100 watts. DC pulse bias with T=5.0 μs and f=15 kHz. The experimental detail was shown as table 3.3.

Table 3.3 Gas flow rate, working pressure and treatment time, nitriding by Pinnacle plus power supply.

Experiments	N_2+H_2 flow (sccm)	Pressure (torr)	Time (min)
Exp 127	60	1.0	60
Exp 128	60	1.0	30
Exp 129	70	2.5	60
Exp 130	70	2.5	30
Exp 131	80	3.5	60
Exp 132	80	3.5	30

The working pressure was controlled by gate valve position and gas flow rate. The temperature was increased from room temperature to approximately 210 ˚C at 20 minute later and then nearly stable (for this case, the specimen's temperature should

be more than 210 ˚C). The working pressure varies about ± 0.3 Torr during process. Gate valve position was adjusted between 100 and 104 to keep at working pressure.

After plasma immersion, wait until the temperature lower than 50 ˚C before open the chamber avoid surface oxidation.

3). Plasma nitriding by Cober power supply.

This experiment also used 4% H_2 with N_2 gas for plasma nitriding. The Cober high power pulse generator model 605P was used to bias the holder. The negative voltage of -1.2 kV with 2 μs on time and 10 μs off time was applied to the substrate holder. The experiment setup and conditions were the same as previous experiment, detail shown as table 3.4.

Table 3.4 Gas flow rate, working pressure and treatment time, nitriding by Cober power supply.

Experiments	N_2+H_2 flow (sccm)	Pressure (torr)	Time (min)
Exp 133	60	1.0	60
Exp 134	60	1.0	30
Exp 135	70	2.5	60
Exp 136	70	2.5	30
Exp 137	80	3.5	Fail
Exp 138	70	2.5	45

4). N_2+CH_4 plasma immersion.

This experiment also called nitride carburization. The substrate holder was bias with Cober high power pulse generator. Negative bias was applied at -1.2 kV with 2 μs on time and 14 μs off time. We reduce bias duty cycle, but the voltage still the same as former. Nitrogen (N_2) and methane (CH_4) gases were feed into the chamber to produce plasma. The K-type infrared thermocouple was used for this

experiment. The thermocouple sensor was placed at 15 cm away from the specimens. The working pressure was 2.5 Torr for all experiment. All case carries out with 60 min. The experiment detail was shown as table 3.5.

Table 3.5 Gas flow rate in N_2+CH_4 plasma immersion.

Experiments	N_2 flow (sccm)	CH_4 flow (sccm)
Exp 162	60	10
Exp 163	50	20
Exp 164	40	30
Exp 165	70	0

After surface treatment, the specimens were kept in ambient nitrogen gas. The treated surface was took photograph by optical microscopy and electrical contact resistance were measured. The samples with best interfacial contact resistance (ICR) will be select for corrosion test. The best condition will apply to improve the AISI 304 bipolar plates for PEM fuel cell single cell test.

3.2 Interfacial contact resistance (ICR) measurement

The interfacial contact resistance determined by sandwiching the specimens between two gas diffusion layers. Davies's method for measurement interfacial contact resistance (ICR) between stainless steel and carbon paper was modified (Davies et al., 2000). The idea of this technique was shown as figure 3.5. Toray carbon paper (IGD-H-120) was used in this experiment. Such carbon paper has been used as the electrode backing. An electrical current (1.000 A) was provided via the two copper plates. By measuring the total voltage drop through this setup, while the compaction force was increased, it was possible to calculate the total resistance dependency on the compaction force according to:

$$R = \frac{VA_s}{I} \quad . \qquad (3.1)$$

Where R is the electrical contact resistance, V the voltage drop through the setup, I the current applied and A_s the surface area.

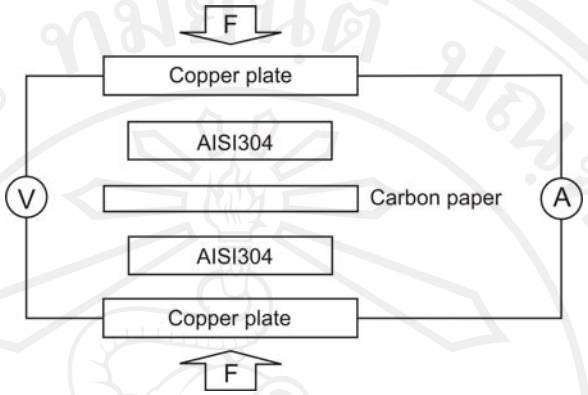

Figure 3.5 Schematic of the test assembly for interfacial contact resistance.

Because the specimen was treated only one side, there are many steps to measure the ICR of treated surface and carbon paper. The experiment procedure shown as follow:

1). ICR of carbon paper and copper plate ($R_{C\text{-}Cu}$).

A carbon paper was sandwiched between two copper plates. An electrical current of 1.000 A was applied via the copper plates through the carbon paper. The definition of voltage drop along the electrical circuit shown as figure 3.6:

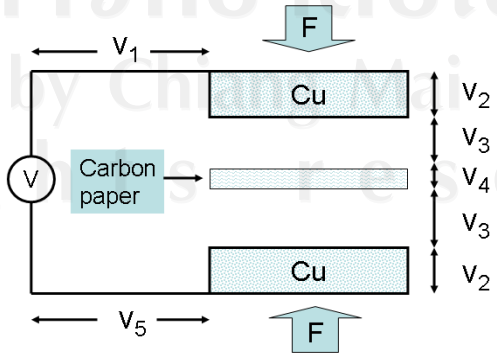

Figure 3.6 Schematic of ICR measurements of carbon paper and copper plate.

There are several resistances in this electrical circuit. By measuring the voltage drop along the circuit, we can calculate the resistance. The voltage would be measured (by FLUKE 189 multi meter) for each compaction force. The compaction force was applied from 10 to 200 N/cm^2. The voltage drop as illustrated in figure 3.6 is then:

$$\begin{aligned} V &= V_1 + 2V_2 + 2V_3 + V_4 + V_5 \\ &= V_1 + 2(IR_{Cu}) + 2V_3 + IR_C + V_5 \end{aligned} \tag{3.2}$$

Where R_{Cu} and R_C are bulk resistance of copper plate and carbon paper respectively. Here we can measured V, V_1 and V_5. So we can calculated V_3. By using equation (3.1), we obtained the ICR of carbon and copper ($R_{C\text{-}Cu}$).

2). ICR of bare AISI304 and copper plate ($R_{SS\text{-}Cu}$).

The experiment setup and calculation is the same as $R_{C\text{-}Cu}$. A piece of bare AISI304 specimen was sandwiched between two copper plates in stead of carbon paper. Similarly, ICR of bare AISI304 and copper plate was obtained using equation (3.1).

3). ICR of treated surface and carbon paper.

The schematic of experimental setup and voltage drop were illustrated in figure 3.7. Now we were known $R_{C\text{-}Cu}$ and $R_{SS\text{-}Cu}$ from the two former steps. The ICR of treated surface and carbon paper will be obtained by calculation (neglect thin film resistance):

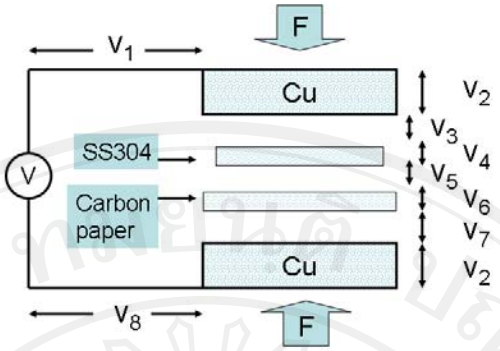

Figure 3.7 Schematic of ICR measurements of specimen and carbon paper.

The voltage of the circuit is then:

$$V = V_1 + 2V_2 + V_3 + V_4 + V_5 + V_6 + V_7 + V_8$$
$$= V_1 + 2(IR_{Cu}) + IR_{SS-Cu} + IR_{SS} + V_5 + IR_C + IR_{C-Cu} + V_8 \quad . \qquad (3.3)$$

Where R_{SS} is bulk resistance of AISI 304 stainless steel,

V_5 is the voltage drop across the contact of treated surface and carbon paper. By using equation (3.1) again, ICR of the specimen and carbon paper was obtained.

For reference, the ICR of ET10 graphite was measured. The ET10 graphite will be used as material for bipolar plates single cell test reference. The specimens with best ICR were selected for corrosion testing. The best experimental condition which had lowest ICR would be used to modified AISI304 fuel cell bipolar plates. The PEM fuel cells with modified bipolar plates were use for single cell test.

3.3 Static water contact angle measurement.

Contact angle, ɵ, is a quantitative measure of the wetting of a solid by a liquid. It is defined geometrically as the angle formed by a liquid at the three phase boundary where a liquid, gas and solid intersect as shown in figure 3.8.

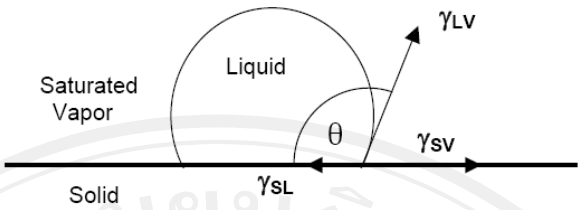

Figure 3.8 A liquid droplet in contact with a solid surface.

Water was dropped from a syringe needle placed on the specimen surface. The image of a water droplet was captured by digital camera and print out by ink jet printer. The contact angle was measured directly from the printed image.

3.4 Corrosion measurement.

The corrosion test was carried out following the ASTM G5 standard (ASTM G5-94). The sample was tested under room temperature with 1 M of sulfuric acid (H_2SO_4) solution without any gas supplied to the corrosion test cell. The surface area of the sample exposed to the solution is 0.785 cm^2. The AgAl was used as reference electrode. The corrosion rate was obtained by SoftCorr III corrosion measurement software. This corrosion test had supported by National Metal and Materials Technology Center (MTEC). The experiment setup was shown in figure 3.9.

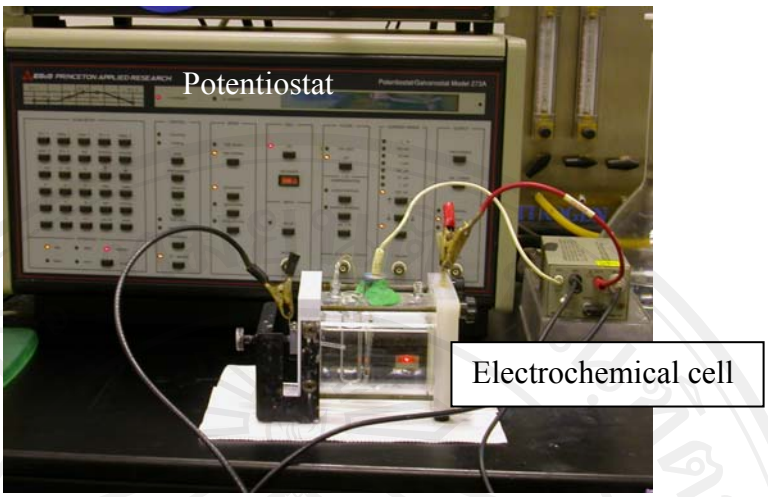

Figure 3.9 Photo of the corrosion test experiment.

3.5 PEM fuel cell single cell test.

AISI304 stainless steel was machined into 25 cm^2 active area bipolar plates, with serpentine flow-field grooves (1 mm wide and 1 mm deep milled grooves). The surfaces of bipolar plates were modified with conditions of the lowest interface contact resistance (ICR) before assembly with commercially membrane electrode assembly (MEA) for single cell test. The MEA was "5L HP Self-Humidifying MEA" with anode and cathode loading of 0.2 and 1.0 mg Pt/cm^2, respectively, on Nafion® 112. Glass-reinforced Teflon® and silicone gaskets of appropriate thickness were used to seal the periphery and provide the desired level of compression on the assembly. The cell was operated at 1 bar and at 65 ˚C. The humidifiers on the anode and cathode side were heated to 64 and 60 ˚C, respectively. Stoichiometry of the fuel and oxidant was 1.5 and 2.0, respectively. Performance of a single cell was evaluated by measuring I-V curves using an electronic load. The ET10 graphite and bare AISI 304 bipolar plates fuel cell were operated at the same condition for reference.

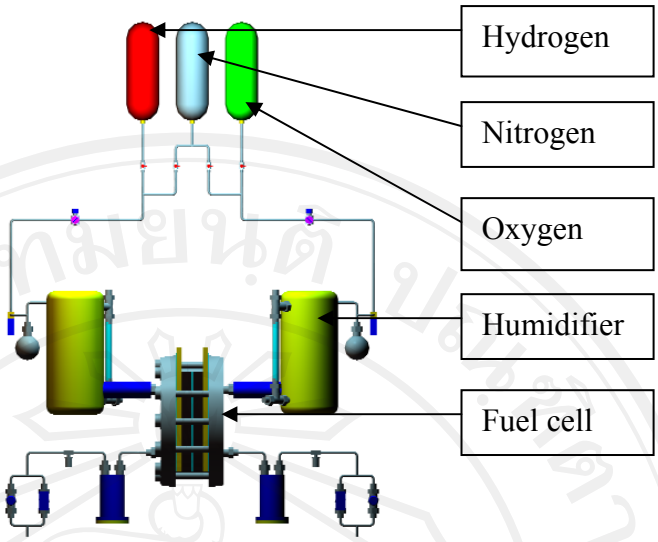

(a)

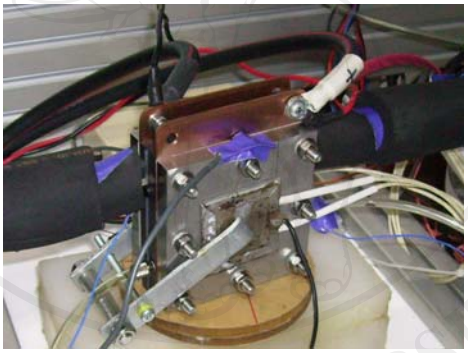

(b)

Figure 3.10 Schematic of fuel cell test experiment set up (a) and a photo of the single cell test (b).